M&C 2017 - International Conference on Mathematics & Computational Methods Applied to Nuclear Science & Engineering, Jeju, Korea, April 16-20, 2017, on USB (2017)

Whole-Core Pin-Resolved PWR Transient Calculations in MPACT

Brendan Kochunas, Ang Zhu, Daniel Jabaay, Yunlin Xu, Thomas Downar

University of Michigan: 1906 Cooley Bldg, 2355 Bonisteel Blvd, Ann Arbor, MI, 48109, bkochuna@umich.edu

Abstract - *This paper describes the validation of the Transient Multi-Level (TML) Method implemented in MPACT using the SPERT III E-Core, and its application to a hypothetical rod ejection transient in a full core Pressurized Water Reactor (PWR) which demonstrates the scalability of the method to full core PWR problems. Preliminary results for the validation of the MPACT for RIA transients using data from test 60 of the SPERT III E-core show very good agreement between experiment and the MPACT prediction. The TML method uses three levels that operate at different temporal and spatial scales. The coarsest time scale and finest spatial scale solves the transient fixed source problem for the transport equation, the intermediate level is based on the Coarse Mesh Finite Difference (CMFD) acceleration method that solves a multi-group diffusion-like equation on a pin-cell based grid. The finest level in time and coarsest in space solves the point kinetics equations. Each level is used to accelerate the solution at the next finest level. The problem analyzed in this work is a PWR based on Watts Bar Unit 1, beginning of cycle 1. One control rod bank is partially ejected to achieve a super-prompt critical transient. The transient is analyzed with and without TML using 5 ms time steps. These solutions are compared to a reference solution generated with a 1 ms time step and no TML. The TML method is shown to provide 3x speed-up over the case without TML and have accuracy consistent with the 1 ms solution. The results confirm the feasibility of performing super-prompt critical transients with MPACT for practical large-scale light water reactor problems.*

I. INTRODUCTION

The Consortium for the Advanced Simulation of Light Water Reactors (CASL) [1] has the goal to solve several challenge problems within the nuclear power industry. One challenge problem is the Reactivity Insertion Accident (RIA) [2].

The RIA is particularly important to the nuclear industry as it presents one of the key, and often limiting, design basis accidents that must be evaluated to meet U.S. Nuclear Regulatory Commission (NRC) licensing requirements. Traditional simulation methods for this type of accident have relied on the diffusion approximation [3]. By advancing the fidelity in the state of the art simulation techniques to pin-resolved spatial kinetics, detailed results of the local energy deposition can be simulated in all pins with local exposure information. This information more accurately identifies the most limiting cases.

The objective of this work is to describe, verify, and demonstrate the methods necessary to perform whole-core, time-dependent, pin-resolved, neutron transport simulations in MPACT. The following section describes the theory underlying the transient calculation in MPACT which is based on the recently developed Transient Multi-Level method (TML) [4]. In the following section, preliminary results are shown for the "test 60" experiment performed in the SPERT III E-core that provide a basis for validating the methodology. Then the results are presented for a hypothetical RIA transient in a PWR based on the Watts Bar Unit 1 model [5]. Finally conclusions for this work are presented and areas of future work are discussed.

II. THEORY

A significant, recent development leveraged in this work to minimize the computational burden for the transient transport calculation was the innovative TML method. It reduces the computational burden for full core transport by using longer time steps for the slowly varying and computationally expensive method of characteristics (MOC) angular flux solution. Smaller time steps are used to capture the more rapidly varying spatial and amplitude flux variations anticipated in an RIA by using the more computationally efficient Coarse Mesh Finite Difference (CMFD) and Point Kinetics (PKE) time-dependent solutions. This method is particularly important for transients such as a super-prompt RIA in which the power changes very rapidly within the first second of the transient, especially for events that begin from the zero power condition. This section summarizes the TML method. For a complete detailed description of the method see [4].

1. 3D Time-dependent Neutron Transport

The time-dependent neutron transport equation is given in Eq. (1) and the precursors in Eq. (2):

$$\begin{aligned}\frac{1}{v(E)}\frac{\partial\varphi(\mathbf{r},\mathbf{\Omega},E,t)}{\partial t} &= -\mathbf{\Omega}\cdot\nabla\varphi(\mathbf{r},\mathbf{\Omega},E,t)\\ &-\Sigma_t(\mathbf{r},E,t)\varphi(\mathbf{r},\mathbf{\Omega},E,t)\\ &+\int_0^{\infty}\int_0^{4\pi}\Sigma_s(\mathbf{r},\mathbf{\Omega}\cdot\mathbf{\Omega}',E'\to E,t)\varphi(\mathbf{r},\mathbf{\Omega}',E',t)d\mathbf{\Omega}'dE'\\ &+\frac{1}{4\pi}\begin{pmatrix}\chi_p(\mathbf{r},E,t)[1-\beta(\mathbf{r},t)]S_F(r,t)\\ +\chi_d(\mathbf{r},E,t)S_d(r,t)\end{pmatrix}\end{aligned}, \quad (1)$$

$$\frac{d\xi_k(\mathbf{r},t)}{dt} = \beta_k(\mathbf{r},t)S_F(\mathbf{r},t) - \lambda_k(\mathbf{r},t)\xi_k(\mathbf{r},t), \quad (2)$$

where φ is the angular flux and ξ_k is the delayed neutron precursor density for delayed group k. S_F and S_d are the fission and delayed neutron sources, respectively. χ_p and χ_d are the prompt and delayed neutron spectrums, respectively, and β is the delayed neutron fraction.

For the discretization of Eq. (1) in time, the commonly used isotropic approximation given by Eq. (3) is employed because of the practical difficulty in storing the time-dependent angular flux. This approximation has been shown to be quite accurate and has been used in several state of the art time dependent transport solvers [6], [7], [8].

$$\frac{\varphi^n(\mathbf{r},\mathbf{\Omega},E) - \varphi^{n-1}(\mathbf{r},\mathbf{\Omega},E)}{v(E)\Delta t^n} \approx \frac{\phi^n(\mathbf{r},\mathbf{\Omega},E) - \phi^{n-1}(\mathbf{r},\mathbf{\Omega},E)}{4\pi v(E)\Delta t^n}. \quad (3)$$

Eq. (2) is solved analytically using a second-order in time approximation for the fission source. This approximation is also commonly used [3].

The superscript *n* in Eq. (3) denotes the time step. Substituting Eq. (3) and the solution of the precursor equations into Eq. (1) and (2), Eq. (1) can be simplified and written as:

$$\begin{aligned}&\mathbf{\Omega}\cdot\nabla\varphi^n(\mathbf{r},\mathbf{\Omega},E) + \Sigma_t^n(\mathbf{r},E)\varphi^n(\mathbf{r},\mathbf{\Omega},E) = \\ &+\int_0^\infty\int_0^{4\pi}\Sigma_s^n(\mathbf{r},\mathbf{\Omega}\cdot\mathbf{\Omega}',E'\to E)\varphi^n(\mathbf{r},\mathbf{\Omega}',E')d\mathbf{\Omega}'dE'\cdot \\ &+\frac{1}{4\pi}\left[\chi^n(\mathbf{r},E)S_F^n(\mathbf{r}) + S_{tr}^n(\mathbf{r},E)\right]\end{aligned} \quad (4)$$

In Eq. (4), χ^n and S_{tr}^n, are given by Eq. (5) and (6).

$$\chi^n(\mathbf{r},E) = \chi_p^n(\mathbf{r},E)(1-\beta(\mathbf{r})) + \chi_d^n(\mathbf{r},E)\beta(\mathbf{r}), \quad (5)$$

$$S_{tr}^n(\mathbf{r},E) = A(\mathbf{r},E)\phi(\mathbf{r},E) + B(\mathbf{r},E)S_F^n(\mathbf{r}) + C(\mathbf{r},E). \quad (6)$$

In Eq. (6). *A* and *B* are the flux and fission source dependent source coefficients, and *C* is a constant coefficient that depends on quantities from the previous time step.

The 2D/1D approximation used in MPACT for steady state calculations [9] may be applied in a straightforward fashion to Eq. (4) to obtain analogous 2D and 1D equations for the time dependent problem. These equations are the discussed in the following subsections.

A. 2D MOC Transient Fixed Source Problem

Integrating Eq. (4) over a finite domain in *z*, and applying the multi-group and discrete ordinates approximations yields the following 2D time dependent fixed source transport equation:

$$\begin{aligned}&\sqrt{1-\mu_m^2}\left(\cos(\alpha_m)\frac{\partial}{\partial x} + \sin(\alpha_m)\frac{\partial}{\partial y}\right)\varphi_{g,m}^{n,z}(x,y) \\ &+\Sigma_{t,g}^{n,z}(x,y)\varphi_{g,m}^{n,z}(x,y) = q_{g,m}^{n,z}(x,y) + \frac{S_{tr,g,m}^{n,z}}{4\pi}\end{aligned}, \quad (7)$$

which is just the 2D steady state equation with an additional transient source term S_{tr}. Here, the superscript *z* denotes averaging over a finite plane, and the subscripts *m* and *g* are the discrete ordinate and group index, respectively; *q* contains the scattering and fission sources along with the axial transverse leakage.

The form of the transient source is the same as Eq. (6), although the *A*, *B*, and *C* coefficients have been averaged over the plane. The coefficient *A* must be weighted by the flux, while *B* is weighted by the fission source.

From here the usual 2D MOC [10] method may applied to Eq. (7) to obtain the numerical solution.

B. 1D Transient Nodal Method

The 1D axial equation is obtained from Eq. (6) in a manner analogous to Eq. (7) except the integration occurs over a finite interval in *x* and *y*. For the conventional 2D/1D approximation the time-dependent multi-group axial equation is:

$$-\frac{d}{dz}D_g^n(z)\frac{d\phi_g^n(z)}{dz} + \Sigma_{t,g}^n(z)\phi_g^n(z) = q_g^n(z) + S_{tr,g}^n(z), \quad (8)$$

where *D* is the diffusion coefficient, *q* is similarly the fission, scattering, and transverse leakage terms. Once again, the transient source, S_{tr}, is of the same form as Eq. (6), only with a different integration than in Eq. (7).

Eq. (8) is solved for each axial segment of a pin-cell in the whole core using the conventional NEM nodal formulation [11]. In MPACT, transient axial nodal kernels based on diffusion and SP3 [12] are available.

C. Transient CMFD Formulation

The CMFD method is a well-developed technique for non-linear diffusion acceleration and has been long used to accelerate transient diffusion based calculations [13]. The concept is to integrate the underlying transport equation over angle and to homogenize onto a coarse spatial grid. Applying this process to Eq. (4) leads to the following balance equation:

$$\sum_s \frac{J^{net,n}_{g,j,s}}{A_{j,s}} + \Sigma^n_{r,g,j}\phi^n_{g,j}V_j = V_j\left(\frac{\chi^n_{g,j}}{k_{eff}}\sum_{g'=1}^{G}\nu\Sigma^n_{f,g'}\phi^n_{g',j} + \sum_{\substack{g'=1\\g'\neq g}}^{G}\Sigma^n_{s,g'\to g}\phi^n_{g',j} + S^n_{tr,g,j}\right), \quad (9)$$

where the subscript j and s denote the coarse cell index and surface on that cell, respectively. V is the cell volume and A is the surface area. For simplicity, Eq. (9) is written in operator notation as:

$$\mathbf{M}\phi = \mathbf{F}\phi + \mathbf{S}\phi + \mathbf{A}\phi + \mathbf{BF}\phi + \mathbf{C}. \quad (10)$$

In Eq. (10), **M** is the leakage and absorption, **F** is the fission source, **S** is the scattering, and **A**, **B**, and **C** correspond to the coefficients in Eq. (6) for the transient source. From here it is easy to see that the transient fixed source may be cast into the following form.

$$(\mathbf{M} - \mathbf{S} - \mathbf{F} - \mathbf{A} - \mathbf{BF})\phi = \mathbf{C}. \quad (11)$$

The above Eq. (11) is the linear system formed and solved in MPACT. The solution of this linear system is obtained using the GMRES solver in PETSc [14] with a block Jacobi preconditioner.

D. Point Kinetics Equations

The point kinetics equations (PKE), given by Eq. (12) and Eq. (13), are obtained by integrating the CMFD precursor equations of Eq. (9) and Eq. (2) using the adjoint flux. The detailed derivation of which is available in other references [15].

$$\frac{dP(t)}{dt} = \frac{\rho(t) - \beta^{eff}_k(t)}{\Lambda(t)}P(t) + \frac{1}{\Lambda_0}\sum_k \lambda^{PK}_k(t)\zeta_k(t), \quad (12)$$

$$\frac{d\zeta_k(t)}{dt} = \frac{\Lambda_0}{\Lambda(t)}\beta^{eff}_k(t)P(t) - \lambda^{PK}_k(t)\zeta_k(t). \quad (13)$$

where P is the power and ζ_k is the adjoint flux weighted precursor concentration for delayed group k. The dynamic reactivity is ρ, β^{eff} is the effective delayed neutron fraction for the integrated system, and Λ is the prompt neutron lifetime, the $_0$ subscript indicates the value at time 0.

The solution of the PKE is obtained by assuming a second-order-in-time shape for the power and integrating Eq. (13) analytically. This solution is substituted into Eq. (12) which is then solved numerically using implicit Euler for the time integration.

2. Simplified Thermal Hydraulic Feedback

The solution of the time-dependent transport equations for practical problems requires the modeling of thermal-hydraulic feedback. In order to assess the performance of the methods here for a Reactivity Initiated Accident (RIA), a simplified thermal hydraulics TH model was developed and implemented in MPACT [16].

Since the most important neutronics aspects of the RIA event typically occur over a very short time range (~secs), the simple internal TH model was found to provide sufficient accuracy. However, the comprehensive modeling of all TH phenomena is available with CTF coupled to MPACT within the CASL core simulator VERA-CS. This section briefly summarizes the simplified TH capability for transient. A more complete description is available in [16].

The simplified TH model employs a 1D convection solution between the coolant and the fuel pins, where the modified Dittus-Bolter correlation proposed in [17] is used to obtain the heat transfer coefficient. Constant pressure is assumed, and thus the axial enthalpy change can be described by the energy conservation. However, this methodology for the convection is only used to obtain steady-state solutions.

A 1D conduction model is used for the heat transfer inside the solid. The thermal conductivity of the cladding comes from [18], and the fuel conductivity correlation is given in [19]. The gap conductivity is set by the user, but a value of 10,000 W/m^2-K is typically used. The conduction calculation is performed for each fuel rod for each axial level. The channels used for the enthalpy calculation can be chosen to be a single rod, quarter assembly, or single assembly.

3. TML Iteration Strategy with Feedback

The overall flow chart for TH feedback in the TML algorithm is shown in Fig. 1, where the three vertical blocks represent the three levels of TML solvers. The left vertical blocks represent the general transport transient iteration scheme with TH feedback, where the angular and sub-pin flux shapes are assumed to be accurate. The pin-wise amplitude function of the transport solution is corrected using intermediate time steps by performing CMFD steps, which is shown in the middle vertical blocks. Similarly, the global shape function predicted by the CMFD steps is assumed to be accurate, and the whole core amplitude is corrected by the fine PKE steps illustrated in the right vertical blocks.

In the present TML iteration scheme, a factor of 5x refinement in the time step is used when going from the transport problem to the CMFD problem, and again when going from the CMFD problem to the PKE problem.

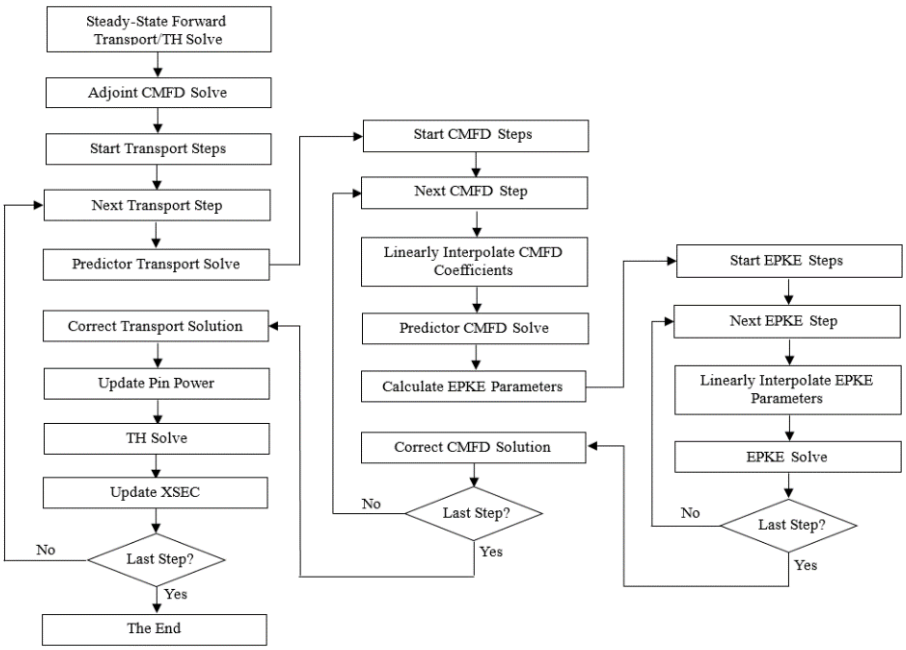

Fig. 1. Flow chart for TML with TH feedback.

III. MPACT TRANSIENT VALIDATION WITH SPERT-E CORE

Initial validation of the MPACT transient capability was performed using a series of experiments from the SPERT-E Core [20]. A schematic of the core is shown in Fig. 2 along with the MPACT model in Fig. 3. The SPERT-E Core consisted of 60 fuel assemblies with 48 of the fuel assemblies containing 25 fuel rods in a 5 by 5 rectangular array, and 12 smaller fuel assemblies each containing 16 fuel rods arranged in a 4 by 4 rectangular array with the same pitch as the 25-rod assemblies.

In previous work, MPACT was validated against KENO for the initial critical conditions at cold zero power and hot zero power [21]. Specifically, preliminary results for the super-prompt critical test 60 are presented. This test is a particularly challenging experiment since the power increases from 50 W to 400 MW within 0.2 seconds. For the simulation of test 60, the TML method is run with 5 ms time steps for the MOC, 2.5 ms for the CMFD time step, and 0.833 ms for the PKE time step. A very coarse MOC discretization is used with 0.05 cm ray spacing, 4 azimuthal angles and 1 polar angle per octant. The 2D/1D solver with the NEM kernel was used and the model was discretized into 20 axial layers. The simplified thermal hydraulics model did not model transient convection, only transient conduction. The control rod decusping uses a pregenerated polynomial. Test 60 was run on the Titan computing cluster at the OLCF [22] on 2,880 processors and took approximately 2 hours.

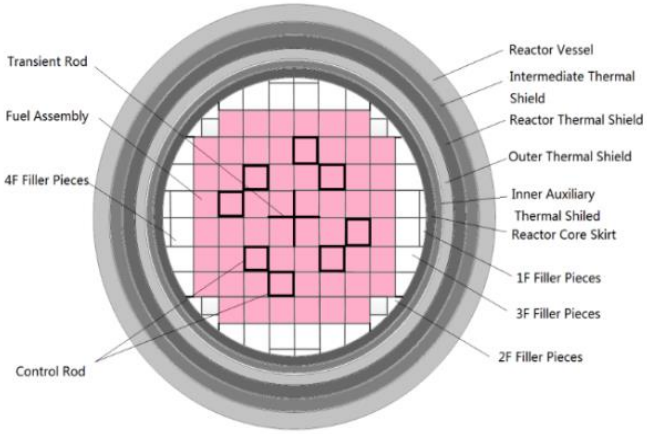

Fig. 2 SPERT E-Core Layout

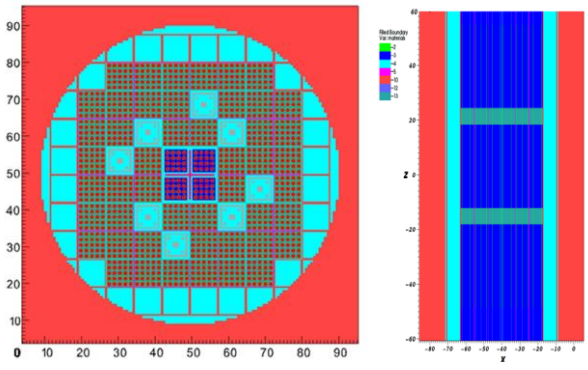

Fig. 3. SPERT-E Core MPACT Model

The total core power and reactivity calculated by MPACT are shown in Fig. 4 and Fig. 5. The relative difference in the peak power and time of the peak are -0.8% and 0.1%, respectively. The difference in the integral of the power pulse is 8.4%. The larger observed difference in the integral of the power pulse may be due to the coarse discretization of the transport problem, the modeling of the rod withdrawal, or control rod decusping model. The agreement between the experiment and simulation for these preliminary results is thought to be quite reasonable at this stage of model development. It is at least as good or better than published results from conventional tools [23],[24].

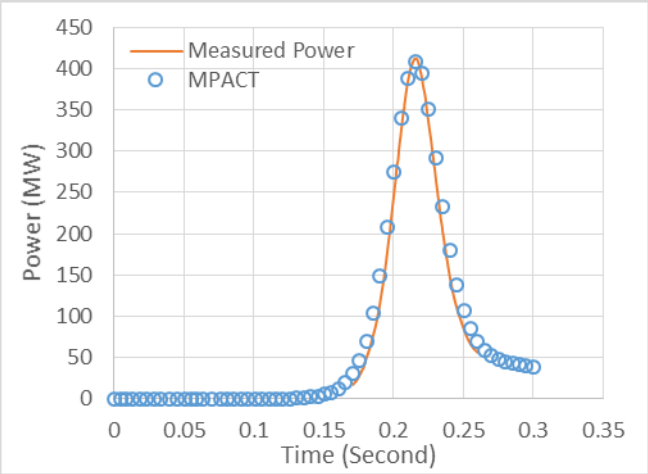

Fig. 4. Test 60 Core Power History

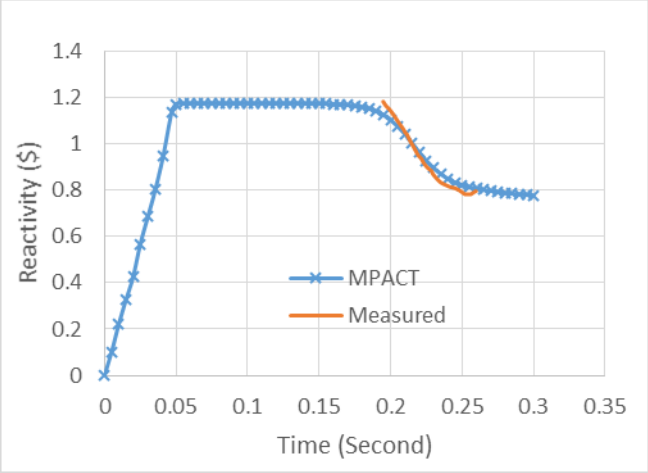

Fig. 5. Test 60 Reactivity History

IV. TRANSIENT SIMULATIONS OF A FULL CORE PWR

The application of interest for the transient methods in MPACT is an operating PWR and the first cycle of Watts Bar I used for the VERA benchmark suite provided a suitable core model for demonstrating the transient capability.

A hypothetical HFP transient with a super-prompt RIA was designed based on the VERA Benchmark problems [5] by partially withdrawing all the control rods in control rod bank D as shown in Fig. 6.

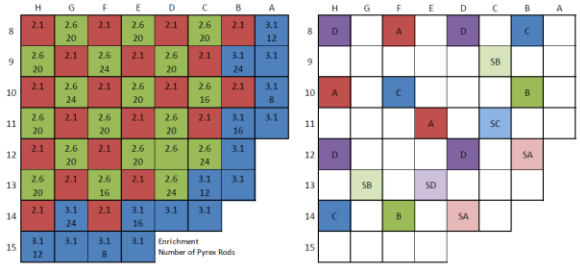

Fig. 6. Watts Bar Unit 1, cycle 1oading pattern and control rod bank layout [5].

The Watts Bar problem is a 3D whole-core model with quarter symmetry and is described in detail in [5], the initial coolant temperature is 565K, the reactor pressure is 2250 psia, and the rated power is 3411 MW, and the rated coolant mass flow is 131.7 Mlbs/hr. For all the calculations performed here, MOC discretization in MPACT is 0.05 cm ray spacing and the Chebyshev-Yamamoto quadrature set [25] using 16 azimuthal and 2 polar angles. The fuel temperature feedback and subgroup resonance treatment were performed at every MOC time step. The case was run with 4234 cores on Eos [26].

In order to assess the accuracy and performance of the TML solution with 5 ms time step for the MOC, a case was run without TML using a 1 ms MOC time step. As shown in Fig. 7, the 1 ms power pulse without TML is closer to the 5 ms with TML, and the change is consistent with previous results [27].

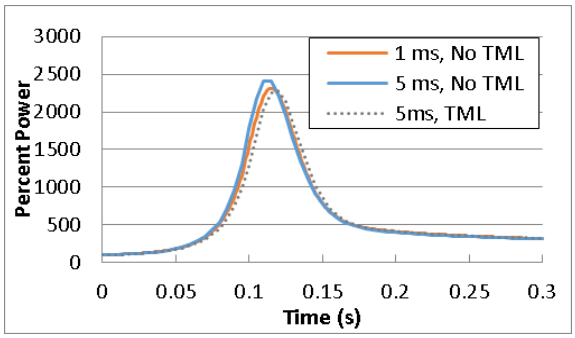

Fig. 7. Bank D Eject with and without TML using 1ms and 5 ms time steps.

In terms of the peak power, the 5 ms no TML case has a relative difference of +4.25% while the TML case has a

relative difference of just -1.25%. The time of the peak compared to the reference case is the same, and the relative difference in the energy deposition is +1.88% for the no TML case and -0.79% for the TML case. The run time for the 1ms time step reference case with only MOC was 8.5 hours; meanwhile the 5 ms time cases with and without TML were 2.5 and 3.33 hours, respectively. Based on the results shown in Fig. 7 and the run times it is reasonable to infer that TML would provide computing time savings of at least a factor of 3 for super-prompt critical transients in Watts Bar without significantly sacrificing solution accuracy.

Fig. 8 shows the radial power distribution at the axial elevation of the peak power during the transient and the axial power for the peak rod during the transient at two different points in time during the transient; Fig. 8(a) is at the beginning of the transient, and Fig. 8(b) is just before the time of the peak core power.

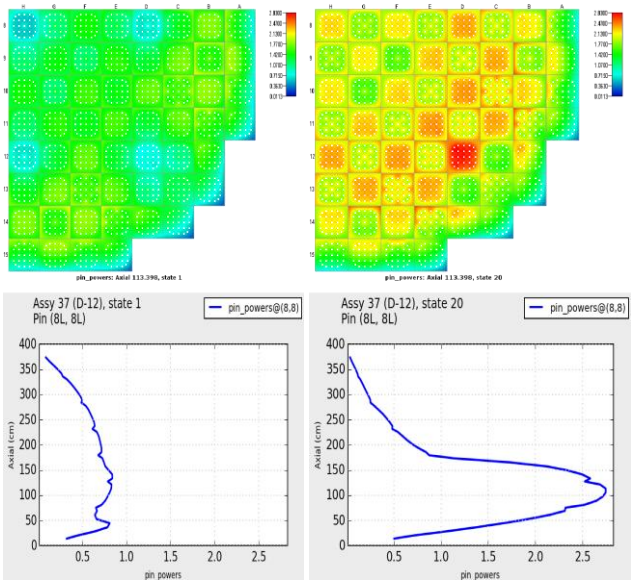

(a) t = 0.005 sec (b) t = 0.100 s

Fig. 8. Power distributions at various times of transient.

V. CONCLUSIONS

The transient formulation for the pin-resolved 2D/1D method was first presented. Then a Transient Multi-Level (TML) method was described which considerably reduces the computational burden for the transient calculation by reducing the frequency of the costly MOC transport calculation. Preliminary results analyzing the SPERT III E-Core test 60 were presented as an initial step towards validation of the transient with promising results. A hypothetical 3D HFP super-prompt transient was designed and simulated for the Watts Bar reactor. The results confirmed the feasibility of performing VERA-CS transients for practical large-scale light water reactor problems.

In future work the focus will be on several tasks necessary to provide the transient capability in VERA-CS for application to the RIA. These include control rod decusping, adaptive time-stepping, coupling with COBRA-TF, and improving the CMFD efficiency.

ACKNOWLEDGMENTS

This research was supported by the Consortium for Advanced Simulation of Light Water Reactors (www.casl.gov), an Energy Innovation Hub (http://www.energy.gov/hubs) for Modeling and Simulation of Nuclear Reactors under U.S. Department of Energy Contract No. DE-AC05-00OR22725. This research also used resources of the Oak Ridge Leadership Computing Facility at the Oak Ridge National Laboratory, which is supported by the Office of Science of the U.S. Department of Energy under Contract No. DE-AC05-00OR22725.

REFERENCES

1. CASL (Consortium for Advanced Simulation of Light Water Reactors), http://www.casl.gov/
2. G. Swindelhurst, "Challenge Problem Implementation Plan: Reactivity Initiated Accident," CASL-I-2013-0060-000, rev 2, January, 2015
3. T. Downar, Y. Xu, and V. Seker, "PARCS v3.0 U.S. NRC Core Neutronics Simulator User/Theory Manual," Depart of Nuclear Engineering and Radiological Sciences, University of Michigan, Ann Arbor, MI, September 2009.
4. A. Zhu, et al., "A Multi-level Quasi-Static Kinetics Method for Pin-Resolved Transport Transient Reactor Analysis", *Nucl. Sci. and Eng.*, 2016, **182**(4).
5. A. Godfrey, "VERA Core Physics Benchmark Progression Problem Specifications," CASL report CASL-U-2012-0131-004.
6. J. Cho, et al., "Transient capability for a MOC-based whole core transport code DeCART," *Trans.Am. Nucl. Soc.*, 2005, **92**, 721.
7. S. Shaner, B. Forget, and K. Smith, "Sensitivity Analysis and Performance of the Adiabatic, Theta, and Multigrid Amplitude Function Kinetics Methods in 2D MOC Neutron Transport," *Proc. M&C 2013*, Sun Valley, ID, May 5-9, (2013).
8. A. Zhu, et al, "Transient Methods For Pin-Resolved Whole Core Transport Using The 2D-1D Methodology In MPACT", *Proc. M&C 2015*, American Nuclear Society, Nashville, TN, USA, April 19-23, (2015)
9. B. Collins, et al., "Stability and Accuracy of Three-Dimensional Neutron Transport Simulations using the 2D/1D Method in MPACT," *J. Comp. Phys.*, **326**, 612-628 (2016).
10. J. Askew, "A Characteristics Formulation of the Neutron Transport Equation in Complicated Geometries," Tech.

Rep. AEEW-R-1108, United Kingdom Atomic Energy Authority (1972).
11. F. Finnemann and M. Wagner, "Interface nodal current technique for multidimensional reactor calculation," *Atomkernenergie*, 1977, **30**:123.
12. S. Stimpson, B. Collins, T. Downar, "Axial Transport Solvers for the 2D/1D Scheme in MPACT." Proc. PHYSOR 2014, Kyoto, Japan (September 28 - October 3, 2014).
13. K. Smith, "Nodal Method Storage Reduction by Nonlinear Iteration," *Trans. Am. Nucl. Soc.*, 1983, **44**:265.
14. S. Balay, et al., PETSc User Manual Revision 3.4 2013.
15. S. Dulla, et al., "Accuracy of a Predictor-Corrector Quasi-Static Method for Space-Time Reactor Dynamics," Proc. PHYSOR 2006, Vancouver, BC, Sept 10-14, (2006).
16. A. Graham, et al., "Assessment of Thermal-Hydraulic Feedback Models," *Proc. PHYSOR 2016*, Sun Valley, Id, May 1-5 (2016).
17. L. Tong and J. Weisman, *Thermal Analysis of Pressurized Water Reactors*, 2nd Ed., Am. Nucl. Soc. (1985).
18. H. Finnemann and A. Galati, "NEACRP 3-D LWR Core Transient Benchmark Final Specifications," OECD Nuclear Energy Agency, NEACRP-L-335 Rev. 1, (1992).
19. D.T. Hagrman et al., "SCDAP/RELAP5/MOD3.1 Code Manual Volume IV: MATPRO -- A Library of Materials Properties for Light-Water-Reactor Accident Analysis," U.S. NRC, NUREG/CR-6150 (1993).
20. J. Durgone, "SPERT III Reactor Facility: E-Core Revision," AEC Research and Development Report, IDO-17036, (1965).
21. L. Cao, et al., "Neutronics modeling of the SPERT III E-Core critical experiments with MPACT and KENO," *Ann. Nucl. Energy*, **80**, pp 207-218 (2015).
22. Oak Ridge Leadership Computing Facility, "Titan" https://www.olcf.ornl.gov/computing-resources/Titan/ (2016).
23. R. Wang, et al., "Validation of the U.S. NRC Coupled Code System TRITON/TRACE/PARCS using the Special Power
24. S. Aoki, et al., "Analysis of the SPERT-III E-Core Using ANCK Code," *J. Nucl. Sci. Technol.*, **46**, pp. 239-251 (2012).
25. A. Yamamoto et al., "Derivation of Optimum Polar Angle Quadrature Set for the Method of Characteristics Based on Approximation Error for the Bickley Function," *J. Nucl. Sci. Technol.*, **44**, pp.129-136 (2007).
26. Oak Ridge Leadership Computing Facility, "Eos" https://www.olcf.ornl.gov/computing-resources/eos/ (2016).
27. A. Zhu, "Transient Methods for Pin-Resolved Whole-Core Neutron Transport," PhD. Dissertation, University of Michigan (2016).